Structure, Vol. 11, 905–913, August, 2003, ©2003 Elsevier Science Ltd. All rights reserved. DOI 10.1016/S0969-2126(03)00134-5

Coupling of Folding and Binding in the PTB Domain of the Signaling Protein Shc

Amjad Farooq,[1,*] Lei Zeng,[1] Kelley S. Yan,[1] Kodi S. Ravichandran,[2] and Ming-Ming Zhou[1,*]
[1]Structural Biology Program
Department of Physiology and Biophysics
Mount Sinai School of Medicine
New York University
New York, New York 10029
[2]Beirne Carter Center for Immunology Research and
Department of Microbiology
University of Virginia
Charlottesville, Virginia 22908

Summary

The notion that certain proteins lack intrinsic globular structure under physiological conditions and that the attainment of fully folded structure only occurs upon the binding of target molecules has been recently gaining popularity. We report here the solution structure of the PTB domain of the signaling protein Shc in the free form. Comparison of this structure with that of the complex form, obtained previously with a phosphopeptide ligand, reveals that the Shc PTB domain is structurally disordered in the free form, particularly around the regions constituting the peptide binding pocket. The binding of the ligand appears to reorganize this pocket through local folding events triggering a conformational switch between the free and the complex forms.

Introduction

Proteins are not static structures but rather represent an ensemble of conformations that are in equilibrium exchange with each other, and such a dynamic system underlies the structural and functional versatility of these molecules. This view is indeed corroborated by several studies in which protein domains have been shown to be wholly or partly unstructured in solution and become structured only upon interaction with their target molecules (Graham et al., 2000; He et al., 2001; Huber and Weis, 2001; Kim et al., 2000; Lei et al., 2000). Disordered regions in particular are very common among proteins encoded by the genomes of higher eukaryotes. Structure prediction studies indicate that as many as one in three eukaryote proteins may be at least partially disordered in the absence of their binding partners (Dunker et al., 2001). Thus, disorder in proteins must be inherently accompanied by an intrinsic functional advantage. One argument that has been put forward is that the conformational heterogeneity resulting from the lack of intrinsic globular structure can in principle account for the binding of the same protein domain to various different target molecules (Dyson and Wright, 2002). In other words, conformational heterogeneity breeds functional versatility in proteins.

In our quest to understand further the role of disorder regions in proteins, we focus here on the phosphotyrosine binding (PTB) domain of the signaling protein Shc from *Homo sapiens*. Shc exists in three distinct isoforms, $p46^{Shc}$, $p52^{Shc}$, and $p66^{Shc}$, which lead to important biological consequences (Figure 1A). While the $p46^{Shc}$ isoform has weak oncogenic cell transformation potential, the $p52^{Shc}$ isoform is highly oncogenic when overexpressed in fibroblasts and can also promote tumor formation through interaction with overexpressed mitogenic receptors or activated kinases (Borrello et al., 1994; Goga et al., 1995; Rozakis-Adcock et al., 1992). Hyperphosphorylation of $p52^{Shc}$ is observed in many different types of tumors (Pelicci et al., 1995; Stevenson and Frackelton, 1998). Cell transformation by polyoma virus middle T-antigen requires its association with $p52^{Shc}$, but not $p46^{Shc}$, via the PTB domain (Dilworth et al., 1994). Furthermore, signaling via insulin receptor (Okada et al., 1995) or the cytosolic protein tyrosine phosphatase PTP-PEST (Habib et al., 1994) is dependent on their binding to the PTB domain of $p52^{Shc}$ but not $p46^{Shc}$.

The PTB domain recognizes activated and tyrosine-phosphorylated receptors containing a phosphotyrosine within the consensus NPXpY motif (Blaikie et al., 1994; Farooq et al., 1999; Kavanaugh and Williams, 1994; Zhou et al., 1995b). These receptors include growth factor, antigen, cytokine, and G protein-coupled and hormone receptors. The PTB domain of Shc binds in a highly specific manner to these receptors and relays the signal to downstream proteins involved in cellular activities such as cell growth, cell differentiation, and apoptosis (Batzer et al., 1995; Batzer et al., 1994; van der Geer et al., 1995; Kremer et al., 1991; Obermeier et al., 1994; Okada et al., 1995; Yokote et al., 1994). For example, binding of the Shc PTB domain to the NPXpY motif within activated receptors, such as TrkA, ErbB2, ErbB3, and EGFR (Obermeier et al., 1993; Pelicci et al., 1992; Ricci et al., 1995), enables the Shc protein to interact with the SH2 domain of the adaptor protein Grb2, which in turn binds via its SH3 domain to the guanine nucleotide exchange factor SOS leading to Ras activation—a protein that orchestrates and links many different signaling pathways within the cell (Rozakis-Adcock et al., 1992; Salcini et al., 1994).

High-resolution structures of PTB domains from several proteins including Shc (Zhou et al., 1995b), IRS1 (Eck et al., 1996; Zhou et al., 1996), X11 (Zhang et al., 1997), Numb (Li et al., 1998; Zwahlen et al., 2000), SNT1 (Dhalluin et al., 2000), and Dab1 (Stolt et al., 2003) in complex with their peptide ligands have been solved and shown to share a common structural fold composed of a central nearly orthogonal antiparallel β sandwich capped at its C terminus by an amphipathic α helix. Larger PTB domains such as those of Shc, Numb, and Dab1 contain accessory structural elements in addition to the central antiparallel β sandwich capped at its C

*Correspondence: amjad.farooq@mssm.edu (A.F.), zhoum@inka.mssm.edu (M.-M.Z.)

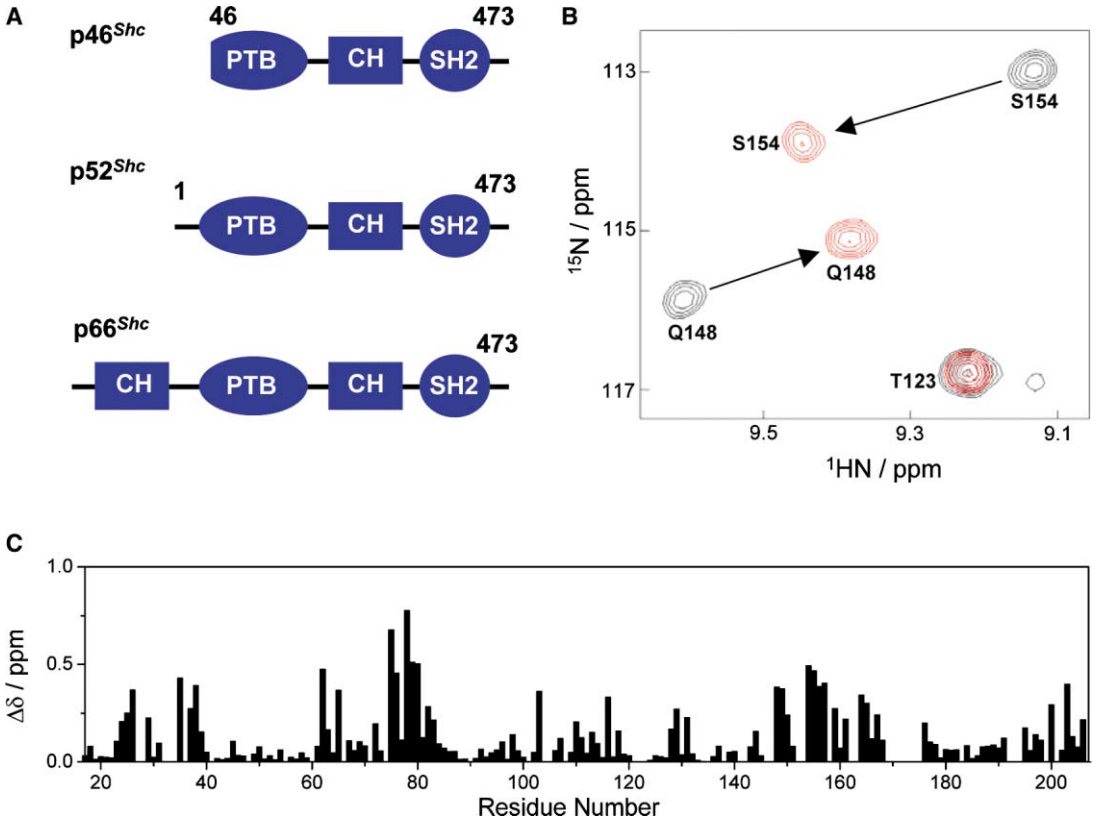

Figure 1. Domain Structure of Shc and the Effects of TrkA Phosphopeptide Binding on the PTB Domain

(A) Alternative splicing of Shc mRNA gives rise to three distinct isoforms: p46^{Shc}, p52^{Shc}, and p66^{Shc}. These differ only to the extent of their N-terminal sequence. All three isoforms contain an N-terminal phosphotyrosine binding (PTB) domain, a central collagen homology (CH) domain, and a C-terminal Src homology 2 (SH2) domain. p66^{Shc} isoform contains an additional CH domain N-terminal to the PTB domain. The PTB domain is mapped to residues 1–207 within the p52^{Shc} isoform.

(B) A superposition of a region of ^{1}H/^{15}N-HSQC showing amide resonances of select residues in the Shc PTB domain (residues 1–207) in the absence (black) and presence (red) of TrkA phosphopeptide, at a protein to peptide molar ratio of 1:1.

(C) A plot of the difference in the chemical shift values ($\Delta\delta$) of the backbone ^{1}HN and ^{15}N resonances of the Shc PTB domain (residues 17–207) in the free form and complexed to TrkA phosphopeptide as a function of residue number. $\Delta\delta$ for each residue was calculated from the equation $\Delta\delta = [(\Delta\delta_{1HN})^2 + (\Delta\delta_{15N}/5)^2]^{1/2}$, where $\Delta\delta_{1HN}$ and $\Delta\delta_{15N}$ are the chemical shift differences in the ^{1}HN and the ^{15}N resonances of the free and the complex forms, respectively, as observed in the ^{1}H/^{15}N-HSQC spectra of the Shc PTB domain.

terminus by an α helix. An interesting observation to note is that the crystal structures of the IRS-1 PTB domain in the liganded and unliganded forms indicate that there are small but significant differences in the two forms (Eck et al., 1996). These are largely concentrated in the loop connecting strands β3 and β4 and in the C-terminal α helix, which interacts with the ligand. The loop β3-β4 appears to be more flexible, while the C-terminal α helix is one turn shorter in the unliganded form. Additionally, the penultimate turn of this helix is also poorly ordered in the unliganded structure. To what extent ligand binding controls the formation of the intrinsic globular fold in the case of other PTB domains has, however, not been addressed. This is particularly relevant in light of the fact that partial structural disordering may be more prevalent in the case of larger PTB domains in the absence of ligand.

In this study, we report a high-resolution solution structure of the Shc PTB domain in the free form and compare it to the structure of the complex form obtained previously (Zhou et al., 1995b). Our data show that the free form is severely disordered in the absence of its peptide ligand and that the binding pocket is only constructed upon the binding of the peptide leading to a more compact fold in the complex form. How coupling of folding and binding appears to be a key event in Shc PTB domain function and implications of this study on possible disorder regions in other PTB domains are discussed.

Results and Discussion

Peptide Binding

The Shc PTB domain is mapped to residues 1–207 at the N terminus of the p52 isoform of Shc protein (Figure 1A). The structure of the Shc PTB domain in complex with a 12 residue tyrosine-phosphorylated peptide (HIIENPQpYFSDA), derived from the Shc binding site of the nerve growth factor receptor TrKA, reveals that the structured core region of the domain is composed of residues 40–199, while residues at both the N and C termini outside this core region are largely unstructured

Table 1. NMR Statistics for the Free Structure of the Shc PTB Domain (Construct 17–207)

Total experimental restraints		2273	
Total NOE distance restraints		2059	
Ambiguous		85	
Unambiguous		1974	
Manually assigned		1155	
ARIA assigned		819	
Intraresidue		902	
Interresidue		1072	
Sequential	$\|i - j\| = 1$	362	
Medium	$2 \leq \|i - j\| \leq 4$	181	
Long range	$\|i - j\| > 4$	529	
Hydrogen bond restraints		102	
Dihedral angle restraints		112	
Final energies (kcal/mol)[a]			
E_{TOT}		131.8 ± 25.8	
E_{NOE}		26.4 ± 10.9	
E_{DIH}		0.7 ± 0.7	
E_{LJ}[b]		−780.5 ± 23.2	
Ramachandran Plot (%)[a]		Full Molecule[d]	Secondary Structure[e]
Most favorable region		62.3 ± 2.7	93.5 ± 2.8
Additionally allowed region		27.0 ± 2.5	6.5 ± 2.8
Generously allowed region		7.3 ± 1.6	0.0 ± 0.0
Disallowed region		3.4 ± 1.3	0.0 ± 0.0
Cartesian Coordinate Rmsd's (Å)[a,c]			
Backbone		1.15 ± 0.10	0.53 ± 0.05
Side chain		1.86 ± 0.11	1.12 ± 0.10

[a] Based upon the 20 lowest energy-minimized structures.
[b] The Lennard-Jones potential was not used during any refinement stage.
[c] None of these final structures exhibit NOE-derived distance restraint violations greater than 0.5 Å or dihedral angle restraint violations greater than 5°.
[d] Residues 42–191.
[e] Residues 42–46, 50–57, 59–62, 74–88, 111–114, 120–127, 130–135, 140–143, 164–169, 175–181, and 187–191.

(Zhou et al., 1995b). The extent to which this structural fold is dependent upon peptide binding, however, remains largely obscure.

On the basis of chemical shift dispersion of backbone amide resonances in the two-dimensional $^{1}H/^{15}N$ heteronuclear single quantum coherence ($^{1}H/^{15}N$-HSQC) spectra, the free Shc PTB domain appears to be structurally folded. Comparison of $^{1}H/^{15}N$-HSQC spectra of the Shc PTB domain in the free form and in complex with TrkA phosphopeptide indicated that a large number of amide resonances, corresponding to residues directly lining the peptide binding pocket as well as in regions remote from it, were significantly perturbed upon peptide binding (Figures 1B and 1C). This salient observation provided a strong indication that the free and the bound forms of the Shc PTB domain may be structurally different. In an effort to fully comprehend these differences, high-resolution three-dimensional structural studies of the free Shc PTB domain were begun.

Structure Determination

The structure of the Shc PTB domain in complex with TrkA peptide was previously obtained using the protein construct composed of residues 17–207 (Zhou et al., 1995b). Thus, to ensure that any structural differences observed between the free and the bound forms of the domain are not due to the differences in the construct, we also used the protein construct 17–207 in our current studies of the free domain. The construct was expressed in bacterial hosts, and various isotopically (^{2}H, ^{13}C, and ^{15}N) labeled protein samples were purified using affinity chromatography on a nickel-IDA column, as described in Experimental Procedures. The backbone and side chain resonances of the protein were assigned from standard heteronuclear three-dimensional triple-resonance nuclear magnetic resonance (NMR) experiments (Sattler et al., 1999; Yamazaki et al., 1994). The structure of the free Shc PTB domain was determined from a total of 2273 NMR-derived distance, hydrogen bonding, and torsional angle restraints (Table 1). A majority of distance restraints were manually assigned, although ARIA was also used in the later stages of the calculation. ARIA-assigned NOEs were manually checked and confirmed. Unlike the complex form, the core region of the Shc PTB domain in the free form consists of residues 42–191. No NOEs were observed between the N- and C-terminal residues 17–41 and 192–207, and the core region of the domain in the free form of the Shc PTB domain.

In order to provide an assessment of the convergence of the structure of the free Shc PTB domain, superimposition of the core region of a family of 20 energy-minimized structures derived from the NMR restraints is depicted in Figure 2A. All structures exhibit good geometry, with no violations of distance restraints greater than 0.5 Å and no dihedral angle violations larger than 5° (Table 1). The atomic root-mean-square deviations (rmsd's) about the mean coordinate position of the backbone and side chain atoms for the secondary structure elements are 0.53 ± 0.05 Å and 1.12 ± 0.10 Å, respectively. Table 1 provides a detailed statistical analysis of the free structure of the Shc PTB domain obtained from the construct 17–207. Except for the N- and C-terminal

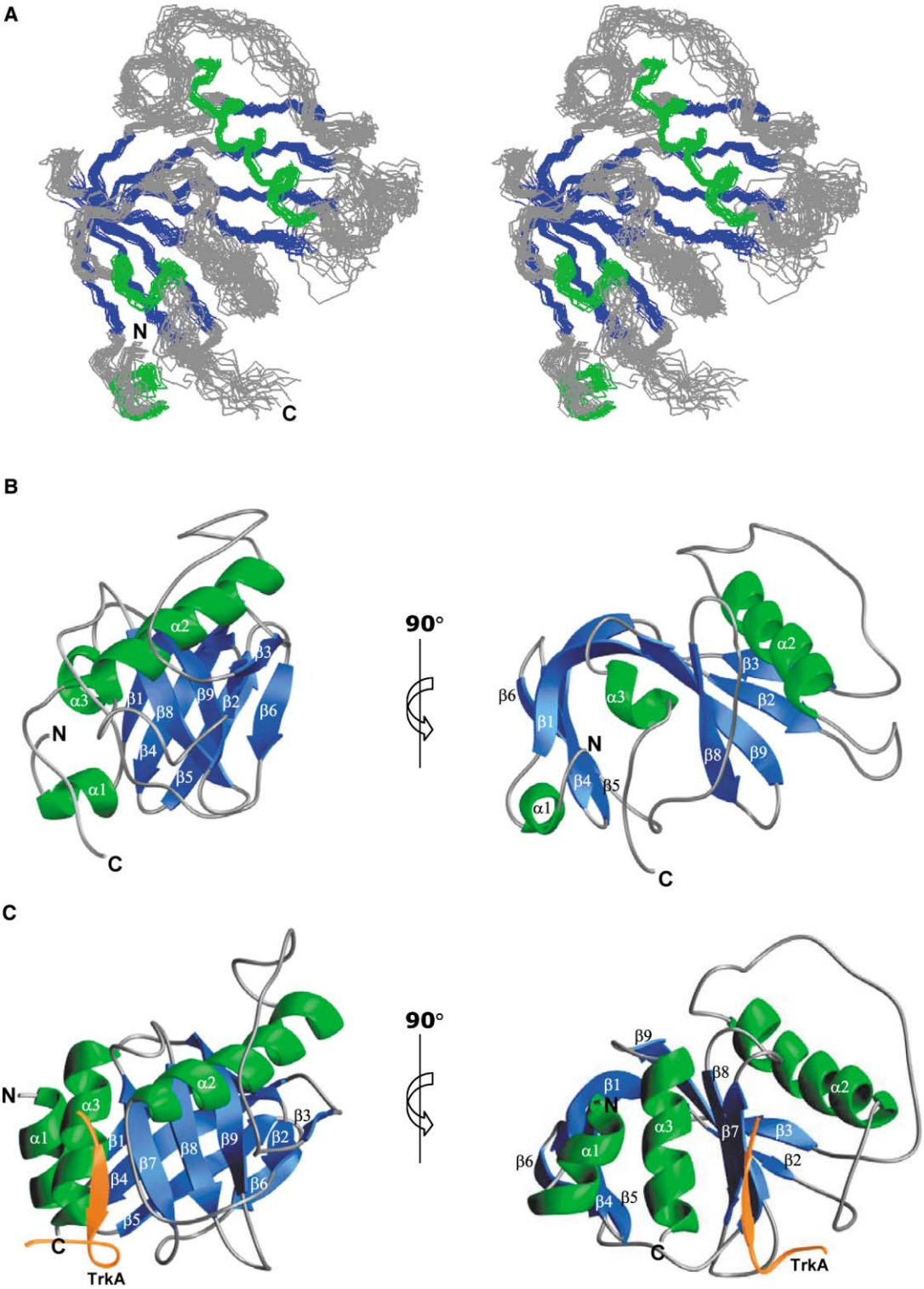

Figure 2. Comparison of NMR Structures of the Shc PTB Domain (Residues 39–200) in the Free and Complex Forms

Structures of both the free and the complex forms of the PTB domain were obtained using a protein construct composed of residues 17–207. For clarity, residues 17–38 and 201–207 in the unstructured regions outside the core domain are omitted. Helices and strands are colored green and blue, respectively. The TrkA phosphopeptide is shown in yellow.

(A) Stereo view of the backbone atoms (N, C^{α}, and C′) of 20 superimposed energy-minimized NMR-derived structures of the Shc PTB domain in the free form.

(B) Two alternative ribbon plots, related by a 90° clockwise rotation about the vertical axis, of the Shc PTB domain in the free form are shown.

(C) Two alternative ribbon plots, related by a 90° clockwise rotation about the vertical axis, of the Shc PTB domain complexed to TrkA phosphopeptide are shown. The orientations of the domain in (B) and (C) are similar. The structure of the Shc PTB domain in complex with TrkA phosphopeptide was obtained previously (Zhou et al., 1995b), and its atomic coordinates can be found under PDB ID code 1SHC.

residues 17–41 and 192–207, the overall structures are well defined.

Given the possibility that the N-terminal residues 1–16 may be structurally important for the Shc PTB domain, we also determined the structure of the construct 1–207 in the free form (data not shown). As expected, the residues 1–41 were structurally disordered and did not appear to have any effect on the structured core region of the domain. In fact, dynamic properties of this N-terminal region broadened and obscured resonances of many residues in the 2D and 3D NMR spectra. The structure of PTB domain from the construct 1–207 was virtually superimposable with that obtained from the construct 17–207 in the free form.

Free Domain Is Structurally Disordered

Figures 2B and 2C compare the ribbon plots of the Shc PTB domain in the free and the complex forms—both determined from the construct 17–207. The structure of the free Shc PTB domain consists of a β sandwich containing two nearly orthogonal antiparallel β sheets and three α helices. As in the complex form (Zhou et al., 1995b), the first β sheet of the β sandwich is composed of strands β1, β4, β5, and β6. However, the second β sheet of the β sandwich only includes strands β2, β3, β8, and β9—the β7 strand that forms an intramolecular antiparallel sheet with β8 and an intermolecular antiparallel sheet with the TrkA phosphopeptide in the complex form is structurally disordered in the free form of the Shc PTB domain.

Apart from the disorder of β7, the β sandwich in the free form is not as tightly packed as it is in the complex form. In the complex form, helices α1 and α3 are packed against one face of the β sandwich creating a hydrophobic cleft for peptide binding. In contrast, these helices undergo partial unwinding of between one and two turns in the free form and are disengaged from creating a hydrophobic cleft necessary for the tight binding of the peptide ligand. The disorder of several key structural elements and the solvent exposure of many hydrophobic residues in the free form are evidence of a partially folded or locally disordered state. How such a structurally disordered state folds into a fully folded structure upon peptide binding is best visualized in the form of a protein movie accessible at http://physbio.mssm.edu/~amjad/movies/shcptb/index.html.

Ligand-Induced Construction of Binding Pocket

It appears that ligand binding plays a critical role in organizing and constructing a hydrophobic pocket necessary for tight peptide binding. Figure 3 shows how the binding pocket becomes severely disrupted and exposed to solvent in the absence of TrkA phosphopeptide. This pocket is composed of an elongated cleft formed by strand β7, the C-terminal helix α3, and the loop connecting β2 and α2 (Figures 2C and 3B). In this cleft, several protein residues including R67, R175, I194, and F198 protrude inward to stabilize the pY (phosphotyrosine) and hydrophobic residues N-terminal to the NPXpY motif within the TrkA phosphopeptide. However, disorder of strand β7 and unwinding of helix α3 (from three turns in the complex form to only one turn in the free form) in the free form not only destroy the cleft necessary for peptide binding but also reposition these key residues involved in protein-peptide interaction away from the binding site (Figures 2B and 3A).

Another important feature to note is the loop β2-α2 that connects the β2 strand to the helix α2 via a smooth right-handed turn in the complexed form (Figures 2C and 3B). This topology of the loop β2-α2 positions R67 at a distance close to pY of the peptide for optimal electrostatic interactions in the complex form. In the free form, however, the loop β2-α2 lacks this local conformation, resulting in R67 being pulled away by at least a few angstroms such that it is no longer optimally positioned to interact with pY (Figures 2B and 3A). Comparison of surface electrostatic potentials of the binding pocket in the free and the complex forms reveals that the latter contains a well-defined hydrophobic groove necessary for tight ligand binding, which is missing in the case of the free form (Figures 3C and 3D).

Model for Coupled Folding and Binding

It has been previously shown that the binding of the Shc PTB domain to phosphopeptides is largely governed by entropic factors (Farooq et al., 1999)—in other words, some sort of conformational change is involved upon the interaction of the two partners. Our structure of the free Shc PTB domain presented here indeed confirms this salient observation. Apart from structural and thermodynamic information, kinetics also presents a powerful tool with which the mechanism of protein-peptide interaction can be deciphered. Although little is known about the kinetics of the binding of the Shc PTB domain to TrKA, studies on a related phosphopeptide with a similar K_d to TrkA indicate that it binds to the Shc PTB domain with a rate constant that is much lower than binding to SH2 domains, which also interact with phosphopeptides in a specific manner (Laminet et al., 1996). Thus, the apparently slower association of Shc may be a virtue of its ability to undergo partial folding in the presence of its peptide ligand.

On the basis of structural, thermodynamic, and kinetic data discussed above, we have taken the step to rationalize the binding of the Shc PTB domain to its peptide ligands in terms of protein folding and binding funnels. We believe that ligand binding to the Shc PTB domain can be explained by two possible scenarios, both of which may be in operation. In the first scenario, the free and the complex forms of the protein are envisaged to respectively occupy local and global energy minima in the protein folding funnel (Figure 4A). These two forms of the protein are structurally distinct. Binding of the ligand to the free form of the protein enables it to overcome the local energy barriers to reach both its fully folded structure and the global energy minima at the bottom of the funnel. The structural changes induced by the ligand would include construction of a peptide binding pocket through local folding events leading to the ordering of the β7 strand and winding of helices α1 and α2. This scenario would be similar to the so-called induced-fit mechanism (Kumar et al., 2000; Ma et al., 1999; Tsai et al., 1999).

In the second scenario, both the free and the complex

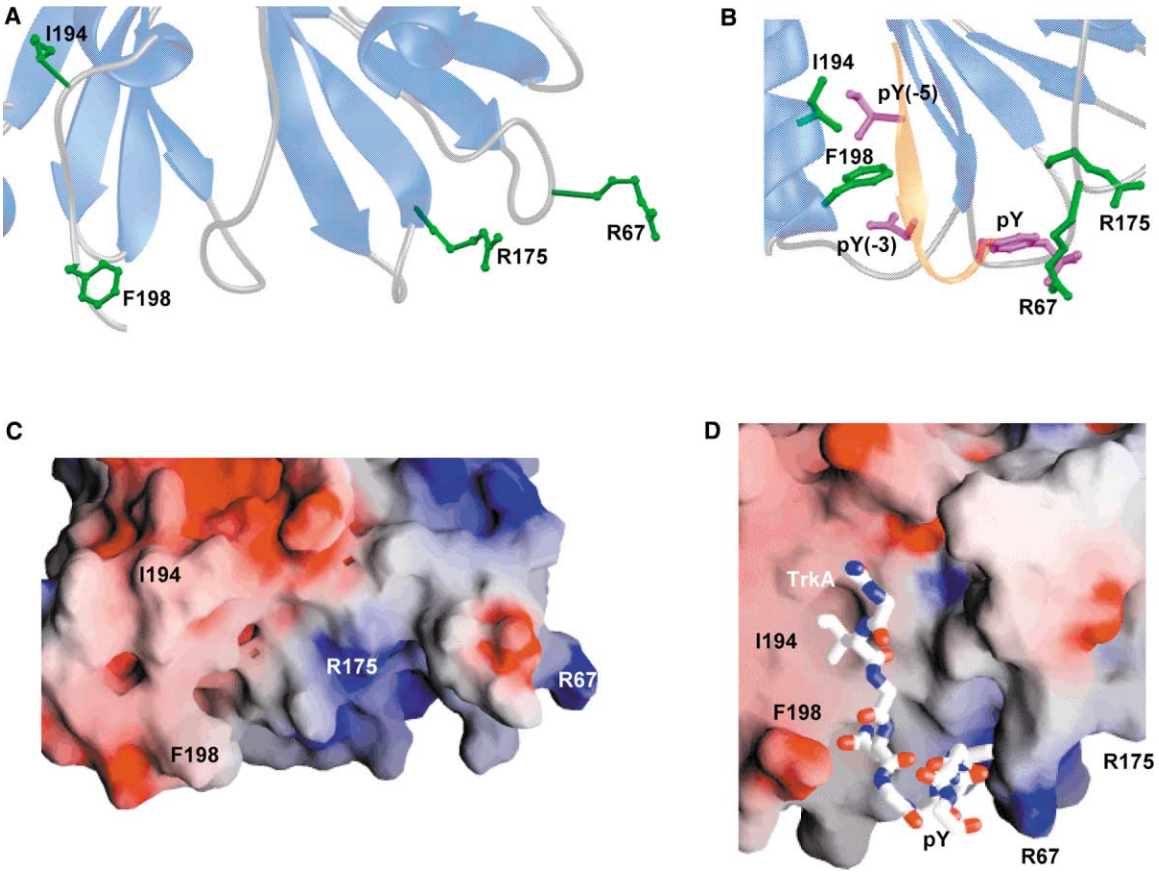

Figure 3. Comparison of the Peptide Binding Pocket in the Free and Complex Forms of the Shc PTB Domain (Residues 39–200)

Key protein residues such as R67, R175, I194, and F198 in the Shc PTB domain that line the peptide binding pocket are shown. Shown are key peptide residues at positions pY(−3) and pY(−5), and pY (phosphotyrosine) in the TrkA phosphopeptide that directly interact with the protein. Also shown are close-up ribbon views of the peptide binding pocket in the free form (A) and the complex form (B), and surface potential views of the peptide binding pocket in the free form (C) and the complex form (D).

forms of the protein would occupy the local energy minima in the folding funnel (Figure 4B). These two forms are considered to be in equilibrium exchange with each other, although the equilibrium is highly in favor of the free form of the protein in the absence of ligand. Ligand only binds to the complex form without any major structural rearrangement of the protein, and allows the complex form to overcome the local energy barriers to reach its global energy minima at the bottom of the funnel. Ligand binding would shift the equilibrium in favor of the complex form such that the free form would undergo the necessary structural changes to become a fully folded structure resembling that of the complex form while still occupying the local energy minima. This situation would be similar to the so-called equilibrium shift mechanism (Kumar et al., 2000; Ma et al., 1999; Tsai et al., 1999).

Biological Implications

The Shc PTB domain links many signaling cascades between activated cell surface receptors and intracellular proteins involved in important biological processes. It has been shown to interact with a distinct set of growth receptors including TrkA, ErbB2, ErbB3, EGF, and insulin receptors (Batzer et al., 1994; Obermeier et al., 1993, 1994). The functional versatility of the Shc PTB domain thus cannot be overemphasized, but how it achieves this does need some illumination. We believe that the structurally disordered state of the free Shc PTB domain may account for its functional versatility, because it would make it much easier for it to be modified accordingly in response to different molecular targets. Given the structural similarity between various functionally different PTB domains, it is conceivable that other PTB domains may also be structurally disordered in their free forms.

The crystal structures of the IRS1 PTB domain in the free and bound forms indicate that the differences between the two forms of the domain are very small compared to those observed here for the Shc PTB domain (Eck et al., 1996). Notably, the loop β3-β4 is less ordered and the C-terminal helix (equivalent to α3 in Shc PTB) is one turn shorter in the free form. IRS1 PTB domain, however, is based on a minimal, central, nearly orthogonal antiparallel β sandwich capped at its C terminus by an amphipathic α helix. Larger PTB domains such as Numb (Li et al., 1998) and Dab1 (Stolt et al., 2003), which structurally resemble the Shc PTB domain and contain

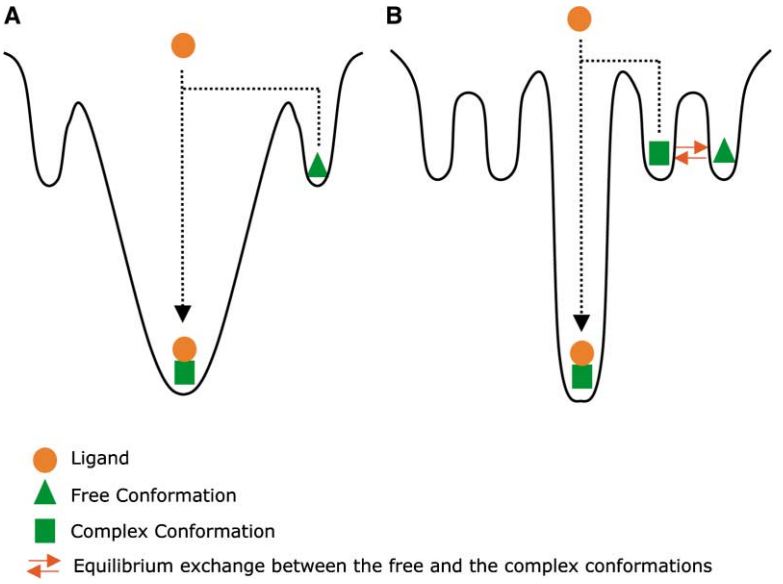

Figure 4. Folding Funnel View of Ligand Binding to the Shc PTB Domain

The vertical axis of the funnel denotes the free energy less the configurational entropy, while the horizontal axis represents the conformational freedom of the protein (indicated by the width of the wells of the funnel).

(A) The free form lies at local energy minima in the absence of ligand. Ligand binding induces structural changes within the free form, allowing it to overcome the local energy barriers to reach the global fold at the bottom of the funnel.

(B) The free and the complex forms coexist in the absence of ligand and are in equilibrium exchange with each other at the local energy minima in the folding funnel. Ligand binding to the complex form allows it to overcome the local energy barriers to reach the global energy minima at the bottom of the funnel, while at the same time shifts the equilibrium from the free to the complex form.

accessory structural elements in addition to the common central β sandwich capped at its C terminus by an α helix, may be prone to significant disorder in the absence of ligand. In fact, our ongoing studies on the SNT PTB domain indicate that the free protein appears to be less stable and exhibits poor chemical shift dispersion in the NMR spectra (unpublished data), implying that the domain is likely to be at least partially unstructured in the absence of its peptide ligand. In short, the conformational switch demonstrated by the Shc PTB domain here may be shared by other larger PTB domains such as Numb and Dab1.

Experimental Procedures

Sample Preparation

The Shc PTB domain constructs (residues 1–207 and 17–207) were cloned, expressed, and purified using procedures as described previously (Zhou et al., 1995a, 1995b). Briefly, each cDNA construct was subcloned into the bacterial expression vector pET15b (Novagen) with a His tag at the N terminus of the recombinant protein and expressed in *Escherichia coli* BL21(DE3). The cells were grown to an optical density of about 0.6 prior to induction with 0.5 mM isopropyl-1-thio-β-D-galactopyranoside for 4 hr at 37°C. Uniformly ^{15}N- and ^{15}N/^{13}C-labeled proteins were prepared by growing bacteria in a minimal medium containing $^{15}NH_4Cl$ with or without $^{13}C_6$-glucose. A uniformly ^{15}N/^{13}C-labeled and fractionally deuterated protein sample was prepared by using a medium containing 75% ^2H_2O. After harvesting the bacterial cells, the protein was purified by affinity chromatography on a nickel-IDA column (Invitrogen) prior to treatment with thrombin to remove the His tag. The cleaved protein was over 95% pure as judged by SDS-PAGE analysis. TrkA phosphopeptide was prepared on a MilliGen 9050 peptide synthesizer (Perkin Elmer) with Fmoc/HBTU chemistry. Phosphotyrosine was incorporated using the reagent Fmoc-Tyr(PO_3H_2) with HBTU/HOAt activation. The peptide was purified by reverse-phase high performance liquid chromatography and its purity checked by mass spectrometry.

NMR Spectroscopy

NMR samples typically contained 0.5 mM protein in 50 mM sodium phosphate and 20 mM DTT-d_{10} in $H_2O/^2H_2O$ (9/1) at pH 6.5. All NMR spectra were acquired at 35°C on a 600 MHz or 500 MHz Bruker DRX NMR spectrometer. The backbone and side chain ^{1}H, ^{13}C, and ^{15}N resonances of the protein were assigned using deuterium-decoupled triple-resonance spectra of HNCA, HN(CO)CA, HNCACB, HN(CO)CACB, and (H)C(CO)NH-TOCSY recorded on a uniformly ^{15}N/^{13}C-labeled and fractionally deuterated protein (Sattler et al., 1999; Yamazaki et al., 1994). The side chain assignments were completed with 3D HCCH-TOCSY (Clore and Gronenborn, 1994) data collected from a uniformly ^{15}N/^{13}C-labeled protein. NOE-derived distance restraints were obtained from ^{15}N- or ^{13}C-edited 3D NOESY spectra (Clore and Gronenborn, 1994; Logan et al., 1993). ϕ-angle restraints were determined from $^3J_{HN,H}$ coupling constants measured in a 3D HNHA-*J* spectrum (Clore and Gronenborn, 1994). Slowly exchanging amide protons were identified from a series of 2D ^{15}N-HSQC spectra recorded after the H_2O buffer was changed to ^2H_2O buffer. All NMR spectra were processed with NMRPipe/NMRDraw (Delaglio et al., 1995) and analyzed by NMRView (Johnson and Blevins, 1994).

Structure Calculations

Structures of the free Shc PTB domain were calculated with a distance geometry-simulated annealing protocol using the X-PLOR program (Brunger, 1993). The initial structure calculations were performed using manually assigned NOE-derived distance restraints. Hydrogen bond distance restraints were added at a late stage of structural calculations for residues with characteristic NOE patterns. The converged structures were then used for the iterative automated assignment of the NOE spectra by ARIA (Nilges and O'Donoghue, 1998), which integrates with X-PLOR for structure refinement. The NOE-derived restraints were categorized based on the observed NOE peak intensities. ARIA-assisted assignments were manually checked and confirmed. Hydrogen bond and angular restraints were determined from the 3D HNHA-J experiment and the program TALOS (Cornilescu et al., 1999). For the ensemble of the final 20 NMR structures, no distance or torsional angle restraint was violated by more than 0.5 Å or 5°, respectively.

Acknowledgments

We thank I. Wolf for peptide synthesis and O. Plotnikova for technical advice and support. This work was supported by an American Cancer Society grant to M.-M.Z. A.F. is a recipient of a Wellcome Trust Fellowship.

Received: December 20, 2002
Revised: May 7, 2003
Accepted: May 12, 2003
Published: August 5, 2003

References

Batzer, A.G., Rotin, D., Urena, J.M., Skolnik, E.Y., and Schlessinger, J. (1994). Hierarchy of binding sites for Grb2 and Shc on the epidermal growth factor receptor. Mol. Cell. Biol. *14*, 5192–5201.

Batzer, A.G., Blaikie, P., Nelson, K., Schlessinger, J., and Margolis, B. (1995). The phosphotyrosine interaction domain of Shc binds an LXNPXY motif on the epidermal growth factor receptor. Mol. Cell. Biol. *15*, 4403–4409.

Blaikie, P., Immanuel, D., Wu, J., Li, N., Yajnik, V., and Margolis, B. (1994). A region in Shc distinct from the SH2 domain can bind tyrosine-phosphorylated growth factor receptors. J. Biol. Chem. *269*, 32031–32034.

Borrello, M.G., Pelicci, G., Arighi, E., Filippis, L.D., Greco, A., Bongarzone, I., Rizzetti, M.G., Pelicci, P.G., and Pierotti, M.A. (1994). The oncogenic versions of the Ret and Trk tyrosine kinases bind Shc and Grb2 adaptor proteins. Oncogene *9*, 1661–1668.

Brunger, A.T. (1993). X-PLOR Version 3.1: A System for X-Ray Crystallography and NMR (New Haven, CT: Yale University Press).

Clore, G.M., and Gronenborn, A.M. (1994). Multidimensional heteronuclear nuclear magnetic resonance of proteins. Methods Enzymol. *239*, 349–363.

Cornilescu, G., Delaglio, F., and Bax, A. (1999). Protein backbone angle restraints from searching a database for chemical shift and sequence homology. J. Biomol. NMR *13*, 289–302.

Delaglio, F., Grzesiek, S., Vuister, G.W., Zhu, G., Pfeifer, J., and Bax, A. (1995). NMRPipe: a multidimensional spectral processing system based on UNIX pipes. J. Biomol. NMR *6*, 277–293.

Dhalluin, C., Yan, K.S., Plotnikova, O., Lee, K.W., Zeng, L., Kuti, K., Mujtaba, S., Goldfarb, M.P., and Zhou, M.-M. (2000). Structural basis of SNT PTB domain interactions with distinct neurotrophic receptors. Mol. Cell *6*, 921–929.

Dilworth, S.M., Brewster, C.E.P., Jones, M.D., Lanfrancone, L., Pelicci, G., and Pelicci, P.G. (1994). Transformation by polyoma virus middle T-antigen involves the binding and tyrosine phosphorylation of Shc. Nature *367*, 87–90.

Dunker, A.K., Lawson, J.D., Brown, C.J., Williams, R.M., Romero, P., Oh, J.S., Oldfield, C.J., Campen, A.M., Ratliff, C.M., Hipps, K.W., et al. (2001). Intrinsically disordered protein. J. Mol. Graph. Model. *19*, 26–59.

Dyson, H.J., and Wright, P.E. (2002). Coupling of folding and binding for unstructured proteins. Curr. Opin. Struct. Biol. *12*, 54–60.

Eck, M.J., Dhe-Paganon, S., Trüb, T., Nolte, R., and Shoelson, S.E. (1996). Structure of the IRS-1 PTB domain bound to the juxtamembrane region of the insulin receptor. Cell *85*, 695–705.

Farooq, A., Plotnikova, O., Zeng, L., and Zhou, M.-M. (1999). Phosphotyrosine binding domains of Shc and IRS1 recognize the NPXpY motif in a thermodynamically distinct manner. J. Biol. Chem. *274*, 6114–6121.

Goga, A., McLaughlin, J., Afar, D.E., Saffran, D.C., and Witte, O.N. (1995). Alternative signals to RAS for hematopoietic transformation by the BCR-ABL oncogene. Cell *82*, 981–988.

Graham, T.A., Weaver, C., Mao, F., Kimelman, D., and Xu, W. (2000). Crystal structure of a β-catenin/Tcf complex. Cell *103*, 885–896.

Habib, T., Herrera, R., and Decker, S.J. (1994). Activators of protein kinase C stimulate association of Shc and the PEST tyrosine phosphatase. J. Biol. Chem. *269*, 25243–25246.

He, X.-L., Chow, D.-C., Martick, M.M., and Garcia, K.C. (2001). Allosteric activation of a spring-loaded natriuretic peptide receptor dimer by hormone. Science *293*, 1657–1662.

Huber, A.H., and Weis, W.I. (2001). The structure of the β-catenin/E-cadherin complex and the molecular basis of diverse ligand recognition by β-catenin. Cell *105*, 391–402.

Johnson, B.A., and Blevins, R.A. (1994). NMRView: a computer program for the visualization and analysis of NMR data. J. Biomol. NMR *4*, 603–614.

Kavanaugh, W.M., and Williams, L.T. (1994). An alternative to SH2 domains for binding tyrosine-phosphorylated proteins. Science *266*, 1862–1865.

Kim, A.S., Kakalis, L.T., Abdul-Manan, N., Liu, G.A., and Rosen, M.K. (2000). Autoinhibition and activation mechanisms of the Wiskott-Aldrich syndrome protein. Nature *404*, 151–158.

Kremer, N.E., D'Arcangelo, G., Thomas, S.M., DeMarco, M., Brugge, J.S., and Halegoua, S. (1991). Signal transduction by nerve growth factor and fibroblast growth factor in PC12 cells requires a sequence of src and ras actions. J. Cell Biol. *115*, 809–819.

Kumar, S., Ma, B., Tsai, C.J., Sinha, N., and Nussinov, R. (2000). Folding and binding cascades: dynamic landscapes and population shifts. Protein Sci. *9*, 10–19.

Laminet, A.A., Apell, G., Conroy, L., and Kavanaugh, W.M. (1996). Affinity, specificity, and kinetics of the interaction of the Shc PTB domain with NPXpY motifs of growth factor receptors. J. Biol. Chem. *271*, 264–269.

Lei, M., Lu, W., Meng, W., Parrini, M.C., Eck, M.J., Mayer, B.J., and Harrison, S.C. (2000). Structure of PAK1 in an autoinhibited conformation reveals a multistage activation switch. Cell *102*, 387–397.

Li, S.-C., Zwahlen, C., Vincent, S.J., McGlade, C.J., Kay, L.E., Pawson, T., and Forman-Kay, J.D. (1998). Structure of a Numb PTB domain-peptide complex suggests a basis for diverse binding specificity. Nat. Struct. Biol. *5*, 1075–1083.

Logan, T.M., Olejniczak, E.T., Xu, R.X., and Fesik, S.W. (1993). A general method for assigning NMR spectra of denatured proteins using 3D HC(CO)NH-TOCSY triple resonance experiments. J Biomol NMR *3*, 225–231.

Ma, B., Kumar, S., Tsai, C.-J., and Nussinov, R. (1999). Folding funnels and binding mechanisms. Protein Eng. *12*, 713–720.

Nilges, M., and O'Donoghue, S. (1998). Ambiguous NOEs and automated NOE assignment. Prog. NMR Spectrosc. *32*, 107–139.

Obermeier, A., Lammers, R., Weismuller, K., Schlessinger, J., and Ullrich, A. (1993). Identification of Trk binding sites for Shc and phosphatidylinositol 3′-kinase and formation of a multimeric signaling complex. J. Biol. Chem. *268*, 22963–22966.

Obermeier, A., Bradshaw, R.A., Seedorf, K., Choidas, A., Schlessinger, J., and Ullrich, A. (1994). Neuronal differentiation signals are controlled by nerve growth factor receptor/Trk bindings for Shc and PLCg. EMBO J. *13*, 1585–1590.

Okada, S., Yamauchi, K., and Pessin, J.E. (1995). Shc isoform-specific tyrosine phosphorylation by the insulin and epidermal growth factor receptors. J. Biol. Chem. *270*, 20737–20741.

Pelicci, G., Lanfrancone, L., Grignani, F., McGlade, J., Cavallo, F., Forni, G., Nicoletti, I., Grignani, F., and Pawson, T. (1992). A novel transforming protein (Shc) with an SH2 domain is implicated in mitogenic signal transduction. Cell *70*, 93–104.

Pelicci, G., Lanfrancone, L., Salcini, A.E., Romano, A., Mele, S., Borrello, M.G., Segatto, O., Fiore, P.P.D., and Pelicci, P.G. (1995). Constitutive phosphorylation of Shc proteins in human tumors. Oncogene *11*, 899–907.

Ricci, A., Lanfrancone, L., Chiari, R., Belardo, G., Pertica, C., Natali, P.G., Pelicci, P.G., and Segatto, O. (1995). Analysis of protein-protein interactions involved in the activation of the Shc/Grb-2 pathway by the erbB-2 kinase. Oncogene *11*, 1519–1529.

Rozakis-Adcock, M., McGlade, J., Mbamalu, G., Pelicci, G., Daly, R., Li, W., Batzer, A., Thoma, S., Brugge, J., Pelicci, P.G., et al. (1992). Association of the Shc and Grb2/Sem5 SH2-containing proteins is implicated in activation of the ras pathway by tyrosine kinases. Nature *360*, 689–692.

Salcini, A., McGlade, J., Pelicci, G., Nicoletti, I., Pawson, T., and Pelicci, P. (1994). Formation of Shc-Grb2 complexes is necessary to induce neoplastic transformation by overexpression of Shc proteins. Oncogene *9*, 2827–2836.

Sattler, M., Schleucher, J., and Griesinger, C. (1999). Heteronuclear multidimensional NMR experiments for the structure determination of proteins in solution employing pulsed field gradients. Prog. NMR Spectrosc. *34*, 93–158.

Stevenson, L.E., and Frackelton, A.R.J. (1998). Constitutively tyro-

sine phosphorylated p52 Shc in breast cancer cells: correlation with ErbB2 and p66 Shc expression. Breast Cancer Res. Treat. *49*, 119–128.

Stolt, P.C., Jeon, H., Song, H.K., Herz, J., Eck, M.J., and Blacklow, S.C. (2003). Origins of peptide selectivity and phosphoinositide binding revealed by structures of Disabled-1 PTB domain complexes. Structure *11*, 569–579.

Tsai, C.-J., Ma, B., and Nussinov, R. (1999). Folding and binding cascades: shifts in energy landscapes. Proc. Natl. Acad. Sci. USA *96*, 9970–9972.

van der Geer, P., Wiley, S., Lai, V.K.-M., Olivier, J.P., Gish, G.D., Stephens, R., Kaplan, D., Shoelson, S., and Pawson, T. (1995). A conserved amino-terminal Shc domain binds to activated growth factor receptors and phosphotyrosine-containing peptides. Curr. Biol. *5*, 404–412.

Yamazaki, T., Lee, W., Arrowsmith, C.H., Mahandiram, D.R., and Kay, L.E. (1994). A suite of triple resonance NMR experiments for the backbone assignment of ^{15}N, ^{13}C, ^{2}H labeled proteins with high sensitivity. J. Am. Chem. Soc. *116*, 11655–11666.

Yokote, K., Mori, S., Hansen, K., McGlade, J., Pawson, T., Heldin, C.-H., and Claesson-Welsh, L. (1994). Direct interaction between Shc and the platelet-derived growth factor β-receptor. J. Biol. Chem. *269*, 15337–15343.

Zhang, Z., Lee, C.-H., Mandiyan, V., Borg, J.-P., Margolis, B., Schlessinger, J., and Kuriyan, J. (1997). Sequence-specific recognition of the internalization motif of the Alzheimer's amyloid precursor protein by the X11 PTB domain. EMBO J. *16*, 6141–6150.

Zhou, M.-M., Harlan, J.E., Wade, W., Crosby, S., Ravichandran, K.S., Burakoff, S.J., and Fesik, S.W. (1995a). Binding affinities of tyrosine-phosphorylated peptides to the COOH-terminal SH2 and NH_2-terminal phosphotyrosine binding domain of Shc. J. Biol. Chem. *270*, 31119–31123.

Zhou, M.-M., Ravichandran, K.S., Olejniczak, E.T., Petros, A.P., Meadows, R.P., Sattler, M., Harlan, J.E., Wade, W., Burakoff, S.J., and Fesik, S.W. (1995b). Structure and ligand recognition of the phosphotyrosine binding domain of Shc. Nature *378*, 584–592.

Zhou, M.-M., Huang, B., Olejniczak, E.T., Meadows, R.P., Shuker, S.B., Miyazak, M., Trüb, T., Shoelson, S.E., and Fesik, S.W. (1996). Structural basis of IL-4 receptor phosphopeptide recognition by the IRS-1 PTB domain. Nat. Struct. Biol. *3*, 388–393.

Zwahlen, C., Li, S.-C., Kay, L.E., Pawson, T., and Forman-Kay, J.D. (2000). Multiple modes of peptide recognition by the PTB domain of the cell fate determinant Numb. EMBO J. *19*, 1505–1515.

Accession Numbers

The atomic coordinates of the structures of the free form of the Shc PTB domain have been deposited in the Protein Data Bank under ID codes 1OY2 (construct 17–207) and 1N3H (construct 1–207).